ELMER PRESS

Original Article

J Endocrinol Metab. 2022;12(4-5):146-160

Oral Glucose-Responsive Nanocarrier System for Management of Diabetes

Rahul Maurya[a, b, d], Suman Ramteke[a], Pranay Guru[c], Narendra Kumar Jain[a]

Abstract

Background: The regulation of postprandial blood glucose concentration in a diabetic person is a toilsome task by the conventional approaches. The continuous monitoring and subcutaneous injection of insulin are always imperative for diabetes management. To overcome the hurdle associated with the conventional system, a glucose-responsive nanoparticle (NP)-based approach was developed for oral insulin administration. The objective of the work is the formulation and characterization of a nanocarrier-based bio-responsive, self-regulated oral insulin drug delivery system.

Methods: The mannose ligand-conjugated NPs were prepared by the inotropic gelation method in which insulin and glucose oxidase enclosed alginate nanocarrier cross-linked by tripolyphosphate. The prepared NPs were filled into the enteric-coated capsule and their release profile was determined at different pH and glucose concentrations. NPs were characterized by size distribution, % drug entrapment, enzyme activity, and *in vivo* and *in vitro* drug release studies.

Results: The average size, surface potential, % drug entrapment of optimized NPs were 245.52 ± 3.37 nm, 22.12 ± 2.13, and 76.15±1.3%, respectively. The release of insulin from optimized NPs (GOx-ALG-MCNPs) (98.56±0.06%) occurs only at higher sugar concentrations (≥ 400 mg/dL) and prevents the release at low sugar concentrations (< 100 mg/dL). The enteric capsule shell protected the formulation to the gastric environment upon oral administration and directed them into the intestine. Mucoadhesion characteristics of NPs prolonged intestinal retention to make them available for cellular uptake. Glucose sensitivity and glucose-dependent effect on different pH environments study revealed that NPs released the drug only at higher concentrations of sugar solution while inhibiting the release at normal and lower sugar concentrations. Besides, compared to other prepared formulations, the GOx-ALG-MCNPs displayed controlled insulin release in response to glucose concentration.

Conclusions: An important finding of GOx-ALG-MCNPs is auto-regulating, glucose-responsive behavior imparting a significantly controlled lowering of blood glucose in an animal model. The findings reveal that the developed glucose-responsive NPs may prove to be a potential strategy for oral insulin delivery.

Keywords: Bio-responsive; Diabetes; Insulin; Nanoparticle; Oral delivery

Introduction

Diabetes is a lifestyle disorder wherein glucose metabolism fails to maintain the normal glucose concentration in the body [1]. The basic cause behind diabetes is insufficient secretion of insulin from the β islets of Langerhans cells in the pancreas [2]. Continuous monitoring and subcutaneous injection of insulin are always imperative for diabetes management. The conventional treatment of diabetes in which drug therapy and glucose monitoring do not occur simultaneously is called open-circuit insulin administration. It does not effectively control blood glucose [3]. There are various categories of the drug for the management of type II diabetes. Insulin therapy is a single approach for the management of type I diabetes [4]. Vial and syringe, insulin pen [5], insulin pump, sensor-augmented pump therapy [6], and threshold suspend insulin pump [7] were used for the effective delivery of insulin through the subcutaneous route [8]. Iontophoresis, sonophoresis, microdermal ablation, and Insupatch were made for the delivery of insulin through the trans-dermal route. Aerodose and Nasulin can be inhaled or given by nasal route. Capsulin, Oral-Lyn, and Oral-Recosulin were made for the oral delivery of insulin [9]. The limitations associated with these systems are nonresponsive and non-patient compliance. In the modern era various novel approaches were developed as alternatives to open-loop insulin delivery systems [10]. These techniques sense the level of glucose and release the insulin into the bloodstream [11]. Another approach to obliterating this problem is an artificial pancreas (two external devices that must be carried and connected at all times) like a close-circuit

Manuscript submitted May 4, 2022, accepted June 10, 2022
Published online August 31, 2022

[a]School of Pharmaceutical Sciences, Rajiv Gandhi Proudyogiki Vishvavidyalaya, Bhopal 462033, India
[b]National Ayurveda Research Institute for Panchkarma, Central Council for Research in Ayurvedic Sciences, Kerala 679531, India
[c]Bansal Institute of Science and Technology, Rajiv Gandhi Proudyogiki Vishvavidyalaya, Bhopal 462033, India
[d]Corresponding Author: Rahul Maurya, School of Pharmaceutical Sciences, Rajiv Gandhi Proudyogiki Vishvavidyalaya, Bhopal 462033, India.
Email: mauryabrahul@gmail.com

doi: https://doi.org/10.14740/jem747

insulin administration system. The release was observed with a change in blood sugar level. This would preclude the risk of insulin-induced hypoglycemia, but the system is not patient-friendly [12]. The major challenge associated with this kind of technique was patient compliance and system validation with the physiological condition. An alternative, a chemically controlled glucose-responsive system has created greater attention during the last few decades [12].

To overcome the problem associated with a closed-loop delivery system like the artificial pancreas and to increase patient suitability, it is necessary to design a glucose-responsive self-regulating system. An insulin-conjugated glucose-responsive molecule controls the release of insulin by their structural modification like shrinkage, swelling, and erosion in response to blood sugar [13]. The commonly used responsive molecules are phenylboronic acid [14], and glucose-binding proteins (GBPs) [15]. Various glucose-responsive systems were made by using glucose-responsive molecules and effectively delivered via the intravenous route. As compared to other routes oral route is the most convenient for the patient. The hurdle associated with the oral delivery of protein or peptide drugs is their enzymatic and acidic degradation in gastric pH [16].

The regulation of postprandial blood glucose concentration in a diabetic person is a toilsome task by the conventional approaches. In this study, a glucose-responsive nanoparticle (NP)-based approach was developed for oral insulin administration. The GOx-ALG-MCNPs consist of insulin and glucose oxidase enzymes entrapped in sodium alginate nanocarrier. The presence of mannose at the surface of the system acts as a ligand for a carbohydrate-binding receptor present in gut-associated lymphoid tissue. The carbohydrate-binding receptor such as lectin has carbohydrate recognition protein and multiple domains for binding carbohydrates like mannose, fucose, maltose, etc. [17, 18]. The developed GOx-ALG-MCNPs were kept into the enteric capsule shell which directs the release of the system in the intestine. The microfold cell (M cell) and Peyer's patches present in the lymph node are the most important transport cell of the intestine. The GOx-ALG-MCNPs have prolonged retention in the intestine due to the mucoadhesive characteristics of chitosan and are selectively taken by the receptor-mediated endocytosis via mannose (carbohydrate ligand)-receptors interaction [19].

However, it was reported that chitosan increases the paracellular permeability by tight junction opening between the cells and promotes paracellular transport of NPs. The mucoadhesive property affects the permeability of the mucous membrane and increases the bioavailability of peptides [20, 21]. Finally, the system will reach the systemic circulation via cellular transport. It was proposed that at elevated blood sugar levels consequent acidification will take place by the oxidation of glucose in presence of glucose oxidase. The acidic environment causes dissociation of chitosan that controls insulin release. The variable system was prepared in this experiment such as GOx-ALG-NCs (glucose oxidase enzyme immobilized alginate nanocarrier), MCNPs (mannosylated chitosan nanoparticles), GOx-MCNPs (glucose oxidase mannosylated chitosan nanoparticles), and GOx-ALG-MCNPs (insulin and GOx-ALG-NCs entrapped mannosylated chitosan nanoparticles). GOx-ALG-NCs were designed to immobilize the enzyme to prevent burst release. MCNPs systems were designed to examine the mucoadhesion and cellular uptake characteristics of mannose in comparison to chitosan NPs. Furthermore, the MCNPs system was also used to investigate the bio-responsive characteristic with comparison to GOx-MCNPs and GOx-ALG-MCNPs. The GOx-MCNPs and GOx-ALG-MCNPs differ on the basis of free and immobilized enzymes; both systems were designed to investigate the effect of the free and immobilized enzymes on NPs characteristics in different glucose concentrations.

Materials and Methods

Materials

Chitosan (128 kDa, > 95% degree of deacetylation (DD), mannosylated), glucose oxidase (18.2 IU/mg), and streptozotocin were procured from Sigma Aldrich (USA) while 27.7 IU/mg of recombinant insulin and sodium alginate (viscosity 200 ± 20 mPas) was purchased from Himidia, India.

Preparation of NPs

Preparation of GOx-ALG-NCs

GOx-ALG-NCs were prepared by the reported method [22] with slight modification. GOx (30 mg) was dissolved in 1 mL of pH 5.8 buffer and added drop-wise into the 10 mL of calcium chloride solution (18 mM) and stirred for 1 h at 1,500 rpm. The centrifugation was carried out for the separation of GOx-ALG-NCs; after that, it was washed with distilled water and air-dried. The control NCs were prepared by the same procedure without enzyme. All the experiment was run in triplicate to minimize the experimental error.

Preparation of GOx-ALG-NCs and insulin cross-linked mannosylated chitosan NPs (GOx-ALG-MCNPs)

The inotropic gelation method was used for the preparation of NPs. The formation of NPs occurs due to the ionic interaction between cation mannosylated chitosan (MCs) and anion; sodium tripolyphosphate and GOx-ALG-NCs). MCs were dissolved in acetic acid (1%, v/v) to prepare 5 mg/mL MCs solution. Insulin (200 IU) was added to the MCs solution. A 26.57 mg GOx-ALG-NCs (equivalent to 10 mg free GOx) was dispersed in TPP solution, the resulting solution was added drop-wise into MCs solution with continuous stirring at 400 rpm. The GOx-ALG-MCNPs were separated using centrifugation (Backman colter Max-LT, UK) at 20,000 g (30 min, 6 °C). The schematic representation is given in Figure 1. A similar system was prepared without using GOx-ALG-NCs called MCNPs, another system was prepared by using free enzyme instead of GOx-ALG-NCs called GOx-

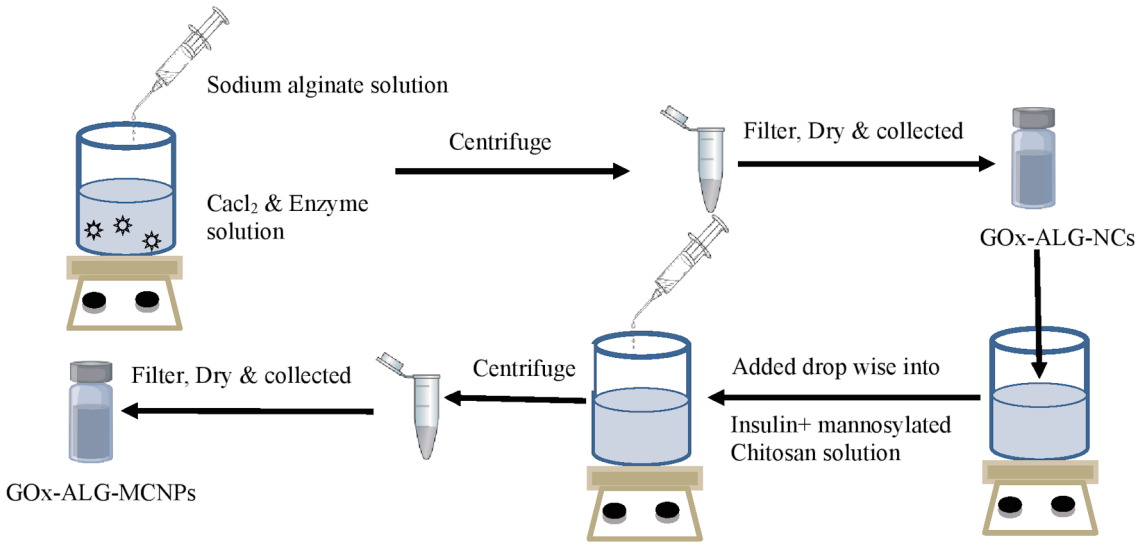

Figure 1. Schematic drawing of the preparation method. Gox-ALG-NCs: glucose oxidase-alginate nanocarriers.

MCNPs. To understand the effect of mannose on cellular uptake study, other NPs were prepared as control by using chitosan instead of mannosylated chitosan, called chitosan nanoparticles (CNPs). The prepared GOx-ALG-MCNPs system was filled into the enteric-coated capsule shell to make them acid-resistant.

Optimization of NPs by experimental design study

The optimization of NPs was carried out by randomized central composite response surface methodology (RSM). The concentration of mannosylated chitosan (1 - 5 mg/mL) and TPP (1 - 3.5 mg/mL) were selected as independent variable. The concentration of GOx-ALG-NCs was kept constant (26.57 mg). The size and entrapment efficiency were selected as dependent response parameters. The experiment was conducted in randomized to minimize error. The Stat-Ease Design-Expert Version13 was used for the statistical analysis of response parameters. The experimental independent parameter and their dependent response parameter are given in Table 1, and the effect of the independent variable on response is mathematically described by the given Equation (1)

$$X = \alpha_0 + \sum \alpha_j X_i + \sum \alpha_{jj} X_{j2} + \sum \alpha_{jk} X_j X_k \quad (1)$$

X exhibited response, α_0 is an intercept, α_j is a linear coefficient, α_{jj} is the square of the coefficient, α_{jk} are interaction coefficient and level of independent variable exhibited by X_i, X_{j2}, X_j, X_k. The analysis of variance (ANOVA) was conducted to determine the model fitness (Fig. 2).

Table 1. Experimental Run and Response

Run	Factor 1, A: MCs (mg/mL)	Factor 2, B: TPP (mg/mL)	Response 1, size (nm)	Response 2, entrapment (%)
1	3	2	188.53	71.26
2	5	2	245.52	76.15
3	3	2	188.53	71.26
4	3	2	188.53	71.26
5	5	3	295.52	71.51
6	1	2	128.28	67
7	1	3	178.81	70
8	3	2	188.53	71.26
9	1	1	168.18	60
10	3	3.5	258.31	73
11	3	1	228.35	64.13
12	5	1	285.52	64.22
13	3	2	188.53	71.26

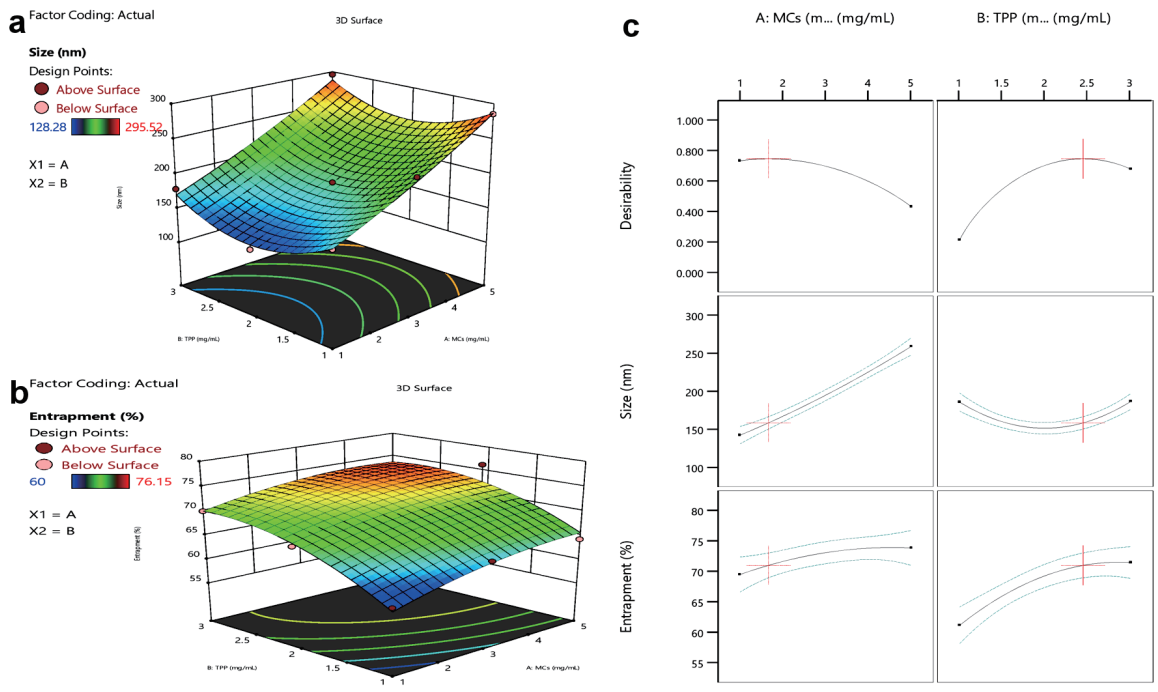

Figure 2. Response surface curve. (a) Size vs. MCs or TPP concentration. (b) Entrapment vs. MCs or TPP concentration. (c) Effect of MCs and TPP on size and entrapment of NPs. MCs: mannosylated chitosan; TPP: tripolyphosphate.

Characterization of NPs

Morphology, particle size distribution, and zeta potential of NPs

Particle size distribution and zeta potential of GOx-ALG-NCs, MCNPs, GOx-MCNPs, and GOx-ALG-MCNPs were performed by dynamic light scattering by using a zeta sizer (Nano ZS, Malvern, UK). Distilled water is used as the dispersion medium. All study was performed in triplicate [23]. Similarly, the size and surface morphology of GOx-ALG-MCNPs were determined by using a scanning electron microscope (Zeiss, Ultra plus, Germany) at an acceleration voltage of 20 kV. Results are shown in Figure 3.

Entrapment efficiency

The entrapment efficiency of GOx in GOx-ALG-NCs and the total protein (GOx and insulin) in GOx-ALG-MNCs were determined by the indirect bicinchoninic acid (BCA) assay method. The GOx-ALG-MCNPs were centrifuged and collected in the supernatant. The amount of unencapsulated protein present in the supernatant was examined by Micro BCA (Thermo Scientific, USA). The insulin-loaded MCNPs, GOx-MCNPs, and GOx-ALG-MCNPs were centrifuged (Backman colter, UK) (14,000 rpm, 30 min); the supernatant was collected to examine insulin content by using high performance liquid chromatography (HPLC) (Shimadzu-I series, Japan) consisting of RP-C18 analytical column, isocratic mode, mobile phase; methanol: 1% acetic acid (60:40, v/v) with the flow rate of 1 mL/min. A quantity of 20 µL sample was injected into the sample injector. The PDA is used as a detector at a wavelength of 276 nm. The concentration of insulin in the injected sample was determined by the developed method with the regression coefficient ($r^2 = 0.99$) [24]. The amount of GOx was determined by subtracting the insulin concentration from the total amount of protein. The drug entrapment efficiency was calculated by the Equation (2).

$$\%EE = \frac{\text{Total Amount of drug added} - \text{free drug in the supernatant}}{\text{Total amount of drug added}} \quad (2)$$

All experiment was done in triplicate and the result were shown in Table 1.

Fourier transform infrared (FT-IR) spectroscopy

The sample (1-2%) (insulin, MCNPs, and GOx-ALG-MCNPs) was separately mixed with KBr, make them fine powder, and placed in a sample holder. The sample was analyzed in the range of 4,000 - 500/cm by FT-IR spectrophotometer (Shimadzu, FT-IR 8700, Japan) at an incident angle of 45° [25]. Results are shown in Figure 4.

Protein structure stability/enzyme activity assay

The stability and activity of the enzyme were analyzed by determining the concentration of product obtained by the

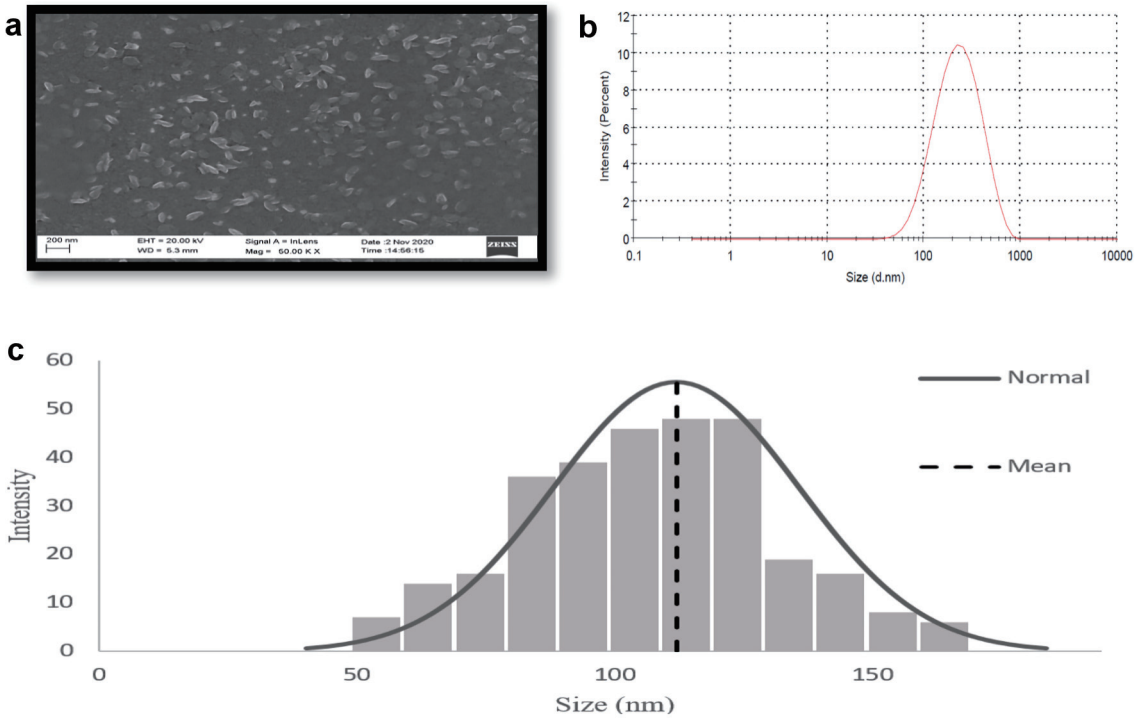

Figure 3. Characterization of GOx-ALG-MCNPs by DLS and SEM. (a) SEM image of GOx-ALG-MCNPs. (b, c) Size distribution study of GOx-ALG-MCNPs measured by DLS and SEM. GOx-ALG-MCNPs: insulin and GOx-ALG-NCs entrapped mannosylated chitosan nanoparticles.

enzyme-substrate reaction. The free and immobilized enzyme (GOx-ALG-MCNPs) was incubated with an equimolar quantity of substrate (glucose) and the concentration of obtained colored product (o-dianisidine) was examined spectrophotometrically (Shimadzu 1800, Japan) at λ = 460 nm (chemical Equations (3) and (4)).

$$\beta\text{ d Glucose} + O_2 + H_2O \xrightarrow{\text{glucose oxidase}} \text{gluconic acid} + H_2O_2 \quad (3)$$

$$H_2O_2 + \text{o-dianisidine (reduced)} \xrightarrow{\text{peroxidase}} \text{dianisidine (oxidized)} + H_2O \quad (4)$$

Typically, 0.1 mL of GOx solution in the range of 50 µg/mL to 300 µg/mL was separately added to 0.3 mL of glucose (18%, w/v) and incubated for 1 min. A similar procedure was repeated with the equivalent amount of GOx-ALG-MCNPs. After the completion of the reaction, the solution was examined at λ = 460 nm and plotted the curve. The slope of the absorbance curve gives information about enzyme activity. Furthermore, to study the effect of pH on enzyme activity, similar experiment was conducted in the different pH conditions of 1.8 to 9.1 (Fig. 5).

Estimation of glucose sensitivity

Swelling studies of MCNPs, GOx-MCNPs, and GOx-ALG-MCNPs were performed in different glucose concentrations (100 - 250 mg/dL) (Fig. 6). Particle sizes of the NPs at different glucose concentrations were determined by using dynamic light scattering; Zetasizer Nano ZS (Malvern Instrument, UK) [26].

Glucose-dependent effect of pH

The pH lowering effect of the enzyme was determined by adding 5 mg of NPs in a 5 mL phosphate buffer (pH 7.4) having glucose concentrations (100 and 400 mg/dL). The pH of the resulting solution was monitored at different time intervals. S1 is an abbreviation for insulin-loaded MCNPs placed in 400 mg/dL glucose solution. S2 and S3 are abbreviations for GOx-MCNPs placed in 100 and 400 mg/dL glucose solution, respectively. S4 and S5 are abbreviations for GOx-ALG-MCNPs placed in 100 and 400 mg/dL glucose solution [27], respectively (Fig. 6).

Ex vivo mucoadhesion and cellular uptake study

Mucoadhesion studies were performed on excised small intestinal tissue of the mice. Excised tissue was cleaned with saline solution then it was opened and fixed to glass support. GOx-ALG-MCNPs were applied over the tissue surface and kept for 15 min. Glass slide was positioned at an angle of 45° and made a constant flow of buffer over it at the rate of 10 mL/min (Fig. 7). The percentage adherence of GOx-ALG-MCNPs on tissue

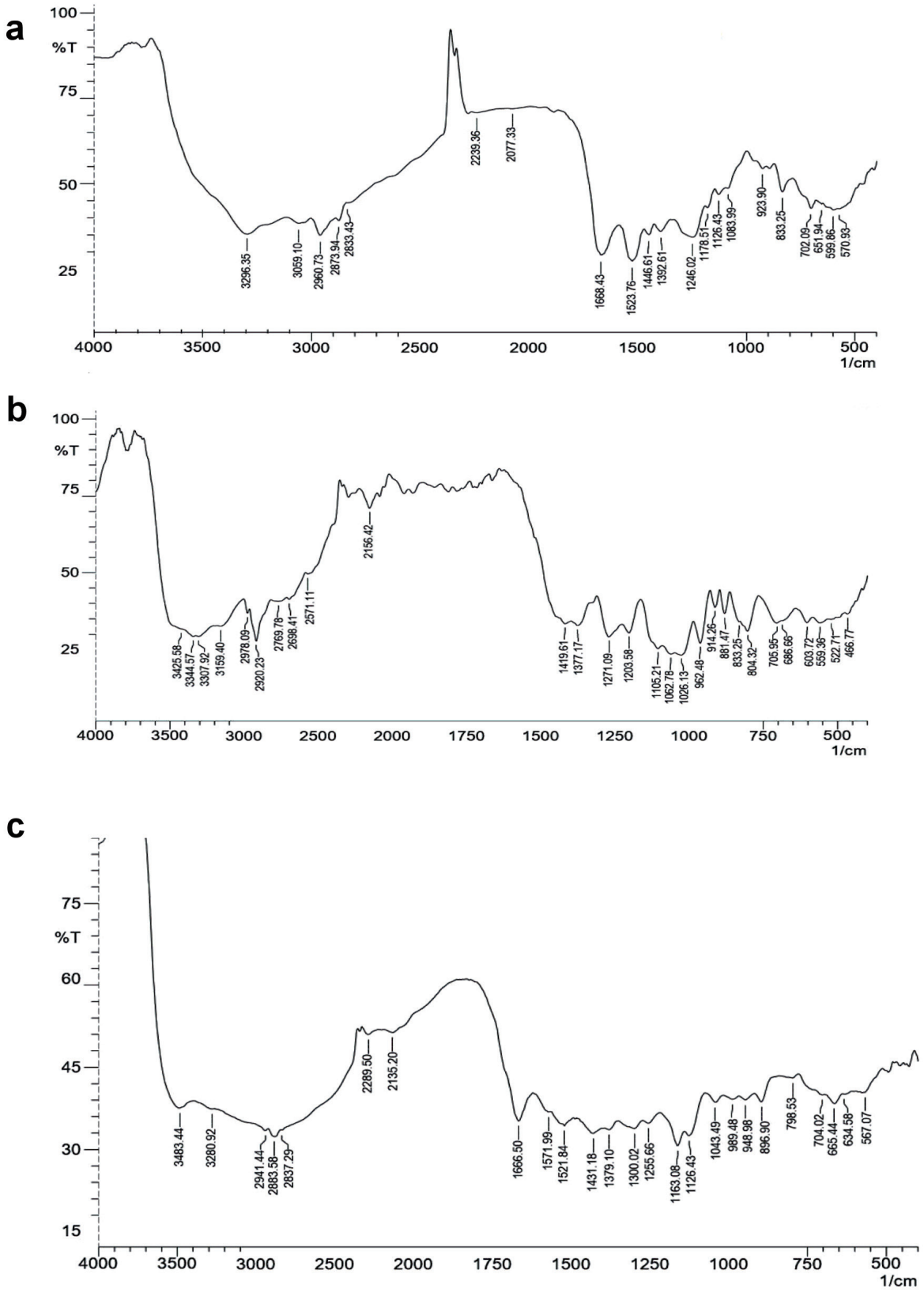

Figure 4. FT-IR spectrum. (a) Insulin. (b) Mannosylated chitosan nanoparticles (MCNPs). (c) Glucose oxidase-alginate-mannosylated chitosan nanoparticles (GOx-ALG-MCNPs). FT-IR: fourier transform infrared.

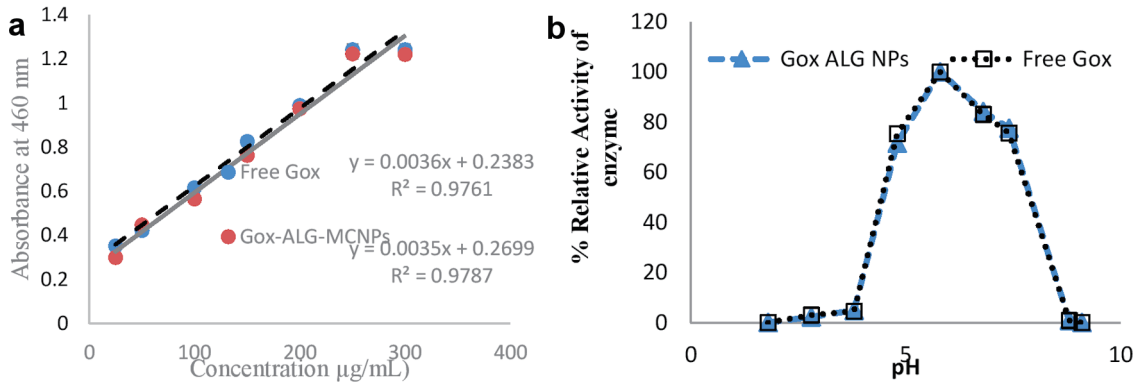

Figure 5. Enzyme activity of the free and entrapped enzyme. (a) Reactivity of different concentrations of free and entrapped enzyme (GOx-ALG-MCNPs) against the fixed concentration of glucose. (b) Effect of pH on % relative activity of the free and entrapped enzyme (GOx-ALG-MCNPs).

surface was determined by the given Equation (5). The cellular uptake study of the different systems was investigated by a histopathological study of the intestinal mucosa. Different formulation CNPs, MCNPs, GOx-MCNPs, GOx-ALG-MCNPs, and one controlled; five histopathological studies were performed on the intestinal mucosa of the mice (Fig. 8).

$$\% \text{ of mucoadhesion} = \frac{\text{Amount retained}}{\text{Amount Applied}} \times 100 \quad (5)$$

In vitro insulin release profile

An *in vitro* drug release study was performed with a slight modification in the reported method [28]. The *in vitro* dissolution of the enteric-coated capsules and the subsequent release profiles of insulin from MCNPs, GOx-MCNPs, and GOx-ALG-MCNPs were investigated in the distinct media simulated to the biological fluid at 37 °C under agitation (100 rpm). The GOx-MCNPs and GOx-ALG-MCNPs were dispersed in a medium consisting of variable (0, 100, and 400 mg/dL) glucose concentrations to study the effect of glucose concentration on the release of insulin. At particular time intervals, test samples were replenished and centrifuged, the supernatants were used for the HPLC analysis. All of the dissolution runs were performed in triplicate. The cumulative amount of insulin released at different time intervals was calculated and plotted against time to obtain the insulin release pattern. The results are shown in Figure 9.

In vivo study/blood glucose lowering effect

The study was conducted as per protocol approved by the Committee for the Purpose of Control and Supervision of Experiments on Animals (CPCSEA) under the reference number PBRI/IACE/08-22/025. The Swiss albino mice were selected for the study. Diabetes was induced in mice by injecting streptozotocin at 50 mg/mL. During the time period of 2 weeks, the mice's blood glucose level reaches up to 400 mg/dL. The mice were kept in fasting conditions during and before 12 h of the experiment, only allowed water. The prepared formulation was administered orally, and blood samples were collected

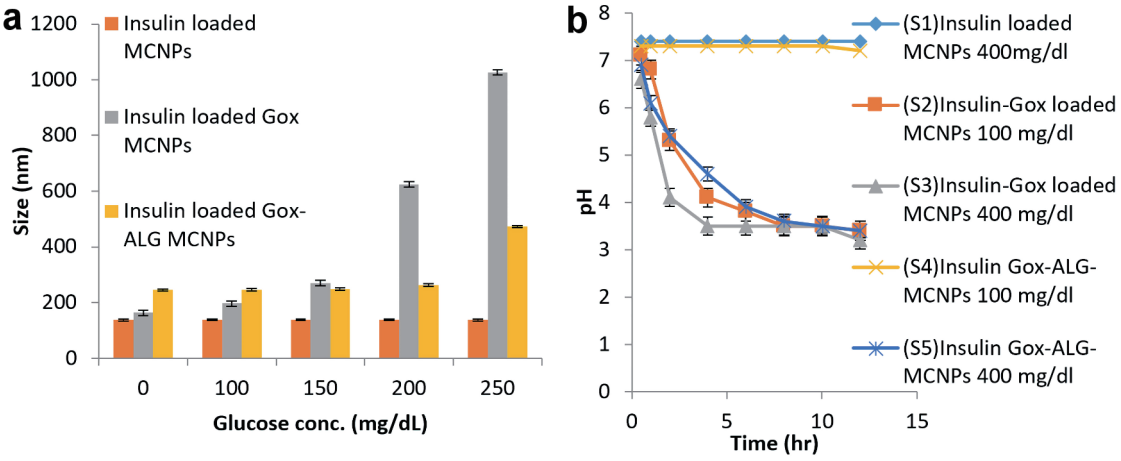

Figure 6. Glucose responsive effect. (a) Swelling or change in size. (b) Lowering of pH at different glucose concentration in different formulations: MCNPs, GOx-MCNPs, and GOx-ALG-MCNPs (mean ± SD, n = 3). SD: standard deviation.

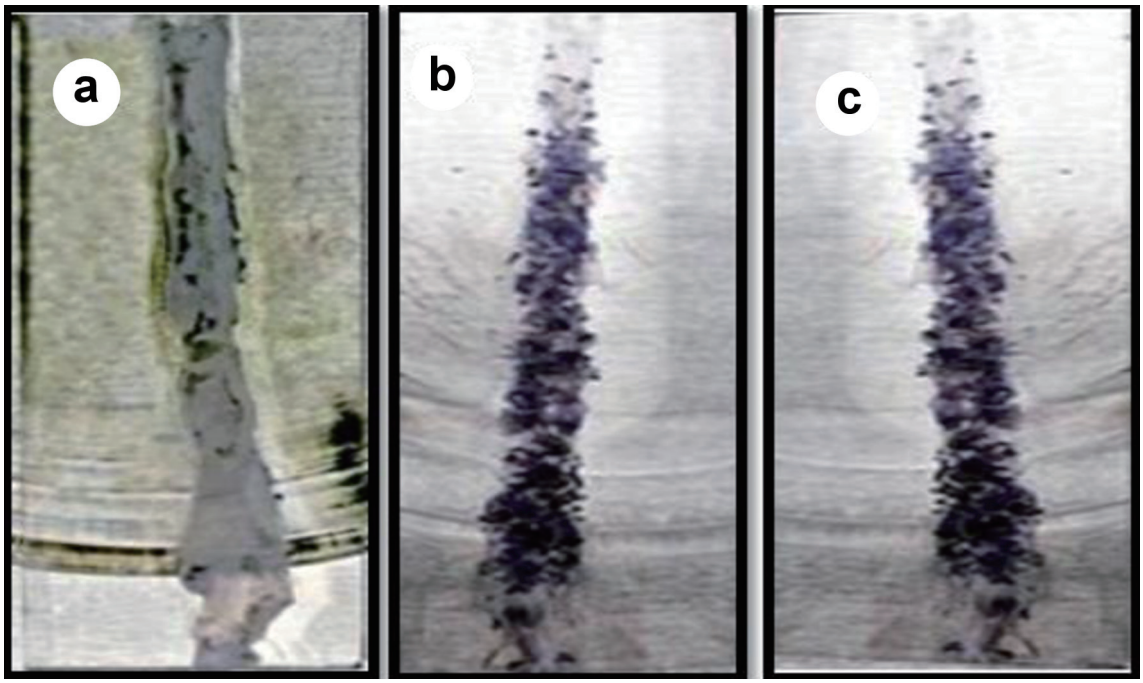

Figure 7. Mucoadhesion of GOx-ALG-MCNPs on the intestine. (a) Before sample application. (b) Sample applied. (c) After washing.

from the tail vein. Mice were divided into 10 groups, and different formulations were given with respect to per kg body weight, Insulin-loaded MCNPs (22.94 mg equivalent to 100 IU), GOx-MCNPs (18.09, 36.19, and 54.28 mg equivalent to 50, 100, and 150 IU insulin, respectively) and GOx-ALG-MCNPs (19.11, 38.23 and 57.35 mg equivalent to 50,100, and150 IU, respectively) were administered. The other group of animals was treated with 50 IU/kg oral insulin and 5 IU/kg subcutaneous injection (control group), and one was kept as a negative control. Blood glucose was examined by a glucometer (Roche instant, India). The observations were recorded in Figure 10.

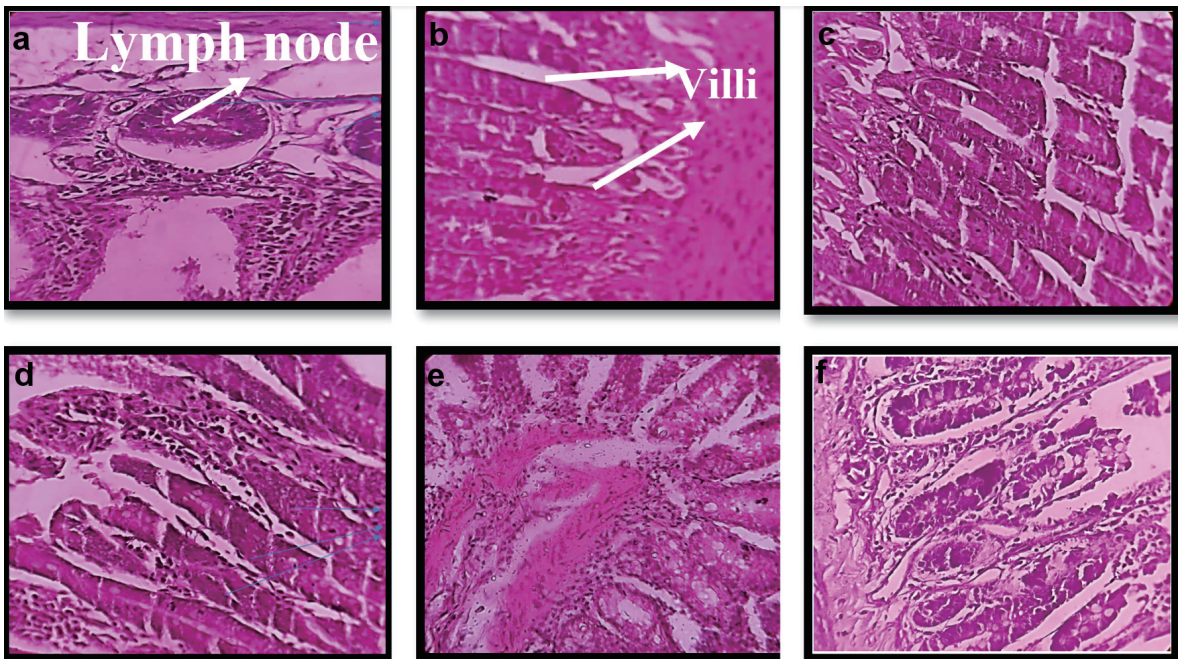

Figure 8. Morphological changes in histopathology of intestinal tissue of mice on treatment with different formulation. (a, b) Normal/control. (c) CNPs treated. (d) MCNPs treated. (e) GOx-MCNPs treated. (f) GOx-ALG-MCNPs treated.

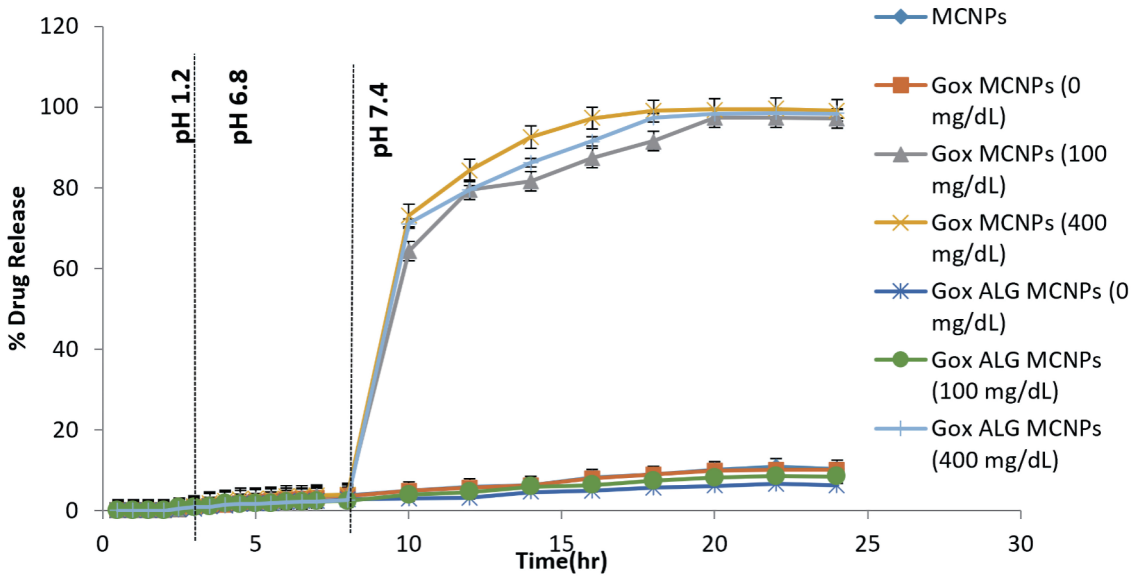

Figure 9. *In vitro* drug release study of different formulations (MCNPs, GOX-MCNPs, and GOx-ALG-MCNPs) in different glucose concentrations (0, 100 and 400 mg/dL) at different pH medium (1.2, 6.8 and 7.4), (mean ± SD, n = 3). SD: standard deviation.

Results and Discussion

Experimental design study

GOx-ALG-MCNPs were prepared by using the randomized central composite RSM. The formulation was optimized on the basis of selected criteria minimum size with maximum entrapment. All the obtained responses were analyzed statically given in Figure 2. The regression coefficient of 0.98 exhibited that the proposed experimental model is reliable. The values of dependent response size were observed in the range of 128.28 to 295.52 nm and entrapment was observed in the range of 60-76.15%. The polynomial Equations (6)and (7) were derived to predict the size and % entrapment of the prepared system.

$$\text{Size} = 251.24 + 20.79 - 138.78\text{TPP} - 0.0786\ \text{MCs} \times \text{TPP} + 1.44\ \text{MCs}^2 + 34.86\ \text{TPP}^2 \quad (6)$$

$$\text{Entrapment} = 41.29 + 4.02\ \text{MCs} + 17.68\text{TPP} - 0.34\ \text{MCs} \times \text{TPP} - 0.35\ \text{MCs}^2 - 3\ \text{TPP}^2 \quad (7)$$

ANOVA study exhibited that independent variable concentrations of MCs and TPP have a significant effect (P value <

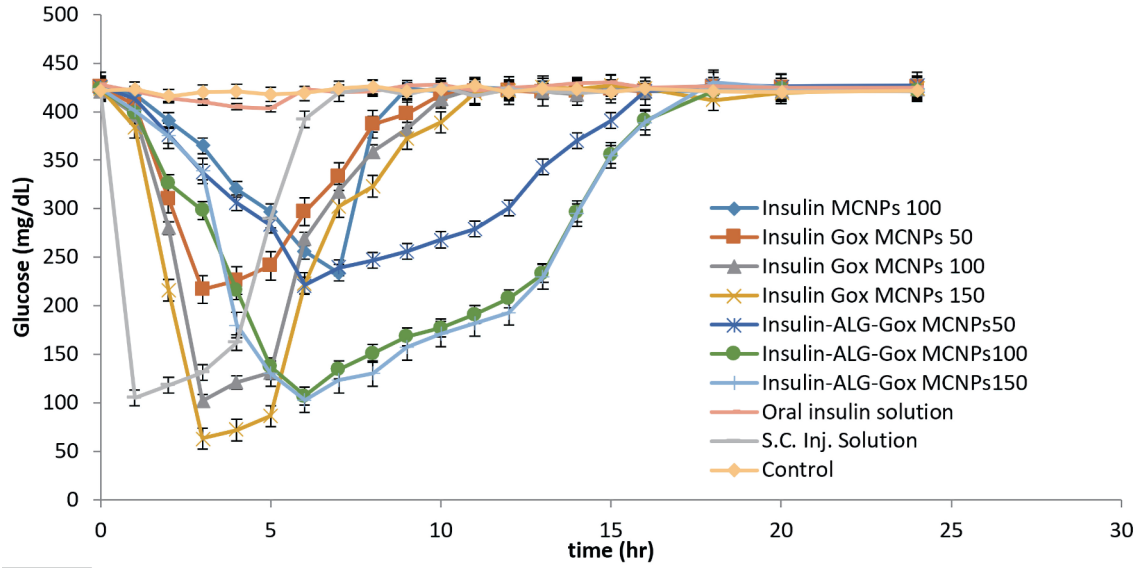

Figure 10. Investigation of the hypoglycemic effect of different oral formulations (MCNPs, GOx-MCNPs, GOx-ALG-MCNPs) and subcutaneous injection on streptozotocin-induced diabetes mice.

Table 2. Size, PDI, and Zeta Potential of Different Formulations

Formulation	Size (nm)	PDI	Zeta potential (mv)	Entrapment efficiency (%)
ALG-NCs	97.23 ± 10.21	0.322 ± 0.013	-6.66 ± 0.67	-
GOx-ALG-NCs	110 ± 11.33	0.361 ± 0.011	-5.41 ± 0.47	88.37 ± 1.3 (GOx)
MCNPs	108.32 ± 6.68	0.214 ± 0.012	26.5 ± 2.31	-
Insulin-loaded MCNPs	137.41 ± 8.12	0.312 ± 0.015	43.5 ± 3.17	81.13 ± 1.6
Insulin-loaded GOx-MCNPs	210.41 ± 8.61	0.261 ± 0.013	28.13 ± 2.31	78.15 ± 1.1
Insulin-loaded GOx-ALG MCNPs	245.52 ± 3.37	0.241 ± 0.009	22.12 ± 2.13	76.15 ± 1.8

Values are represented as mean ± SD (n = 3).

0.05) on dependent response size and % entrapment. The effect of independent variables on response parameters shown in the response curve (Fig. 2), exhibited that size and entrapment of the NPs increase by increasing MCs concentration, but TPP shows a concentration-dependent effect. The minimized size with high entrapment NPs was formed up to 2 mg/mL concentration of TPP. On increasing the concentration > 2 mg/mL, size gradually increases without any significant change in entrapment. TPP regulates the size and entrapment by cross-linking, it is cross-linked with the positively charged amino group of MCs. The elevated TPP concentration above 2 mg/mL decreases the positive amino group of MCs and retards the level of cross-linking; as result large size particles were formed with low entrapment [29]. The high concentration of MCs with a low level of TPP produces poorly cross-linked, non-uniform aggregates. However, at sufficient TPP concentration high degree cross-linking produces small size particles with low PDI and higher entrapment. The experimental run predicted the value of independent variable MCs and TPP was 5 and 2 mg/mL, respectively, and the predicted value of the dependent response size was 248.168 nm, and entrapment was 74.07%. The experiment was conducted in triplicate with the suggested value of an independent variable. The observed response was size (245.52 ± 3.37 nm) and entrapment (76.15±1.8%). The closeness of predicted and observed values exhibited the validation of the experimental design.

Characterization of NPs

Morphology, particle size distribution, and zeta potential of NPs

The size distribution, polydispersity index, and zeta potential of formulations are shown in Table 2. ALG-NCs were developed as a result of the dimerization of alginate chains which gives a gel-like network [30, 31]. The size of GOx-ALG-MCNPs controlled by TPP and MCs, as the amount of TPP, increased up to 2 mg/mL, the degree of cross-linking increased; as a result, the small size with low PDI NPs was formed. Above this concentration, (> 2 mg/mL) precipitation will occur. The size plays a vital role in the cellular uptake of the NPs. The smaller NPs were liable to cross the sub-mucosal layers while the larger size micron-particles were predominantly localized in the epithelial lining [32]. The optimized formulation was obtained at a concentration of 2 mg/mL of TPP and 5 mg/mL of MCs solution. The size of the GOx-ALG-NCs was greater as compared to blank ALG-NCs due to the molecular size of an enzyme. The zeta potential of GOx-ALG-NCs was found to be lower as compared to blank ALG-NCs due to the ionic charge of the protein. The size of GOx-ALG-MCNPs was increased due to the loading of GOx and insulin while the surface potential of GOx-ALG-MCNPs was decreased due to the negative charge of GOx and alginate (Table 2). Figure 3 shows the morphological features of the GOx-ALG-MCNPs. Most of the NPs were found to be oval in shape, and the outer surface of the NPs was smooth and even, similar to the other findings [33, 34]. SEM analysis exhibited that the particle sizes of GOx-ALG-MCNPs formulation varied within a range of 53 to163 nm. The average particle size of the GOx-ALG-MCNPs was found to be 116.15 nm; during DLS analysis, the size is larger because of the measurement of hydrodynamic in this process [35].

Entrapment efficiency

The entrapment efficiency of GOx and insulin was determined by the indirect BCA and HPLC method. The amount of insulin was determined by calculating the AUC of the peak appearing at Rt 5.469 min. The total amount of protein was determined by the BCA method. The amount of GOx was calculated by subtracting the amount of insulin from the total protein. The entrapment efficiency depends on the association of the acidic group of insulin and the amino group of chitosan [36]. From the results, it was evident that size and entrapment increased gradually as the concentration of MCs was increased; but the size and entrapment were controlled by the level of cross-linking agent (TPP). Significant size and entrapment were observed at a polymer to TPP ratio of 5:2. The presence of enzyme also affects the size and entrapment efficiency of formulation as shown in Table 1. The yield of the prepared system: GOx-ALG-NCs, MCNPs, GOx-MCNPs, and GOx-ALG-MCNPs were 70.43 ± 1.54, 37.23 ± 1.21, 56.57 ± 1.87, and 58.23 ± 1.36 mg with the entrapment of 88.37±1.3% (26.51 IU glucose oxidase) 81.13±1.6% (162.26 IU), 78.15±1.1% (156.3 IU), and 76.15±1.8% (152.3 IU) insulin respectively. The entrapment efficiency of insulin in the GOx-ALG-MCNPs was low to MCNPs because of the entrapment of dual protein GOx-ALG-NCs and insulin. The entrapment of multiple components slightly increases the size. However, The GOx-ALG-MCNPs system was selected for further investigation

because the mannosylated system can be selectively uptake by receptor-mediated endocytosis [37]; furthermore, the system consists of an immobilized enzyme that plays a significant role in the designing of controlled and responsive drug delivery.

FT-IR spectroscopy

FT-IR spectra of insulin (Fig. 4a) exhibited peaks of the amide group at 1,668 and 1,523/cm. The peak that appeared at 3,296 and 1,446/cm was N-H and C-N stretching of the amide. Aliphatic C-H stretching was confirmed by peaks observed at 2,960 and 2,873/cm [38]. FT-IR spectra of MCNPs (Fig. 4b) exhibited a peak at 804 and 881/cm are the characteristic signal of mannose, COO symmetric, and asymmetric stretching signals observed at 1,419, similar kind of result depicted by Shilakari et al [39]. The carbonyl bond of insulin dimnished indicating MCs overlapping with insulin. FT-IR spectra of GOx-ALG-MCNPs (Fig. 4c) exhibited signals at 1,255 and 989/cm indicating the C-O stretching of alginate [40]. In the FT-IR spectra of the GOx-ALG-MCNPs broadband were observed around 3,500 to 3,000/cm, which illustrated enhanced hydrogen bonding by the interaction of alginate and chitosan [41]. GOx peak gets disappeared due to the overlapping with ALG.

Protein structure ability/enzyme activity assay

The GOx-ALG-MCNPs and free GOx activity were examined through a spectrophotometer at $\lambda = 460$ nm. The intensity of the color is based on the oxidation of glucose [42], shown in equtions (2) and (3) and Figure 5a. The value of enzyme-substrate reaction was plotted and found that the value significantly fitted in the straight line equation $Y = MX + C$, where Y is the absorbance of the colored product of enzyme-substrate reaction and X is the differential concentration of enzyme solution at which catalytic reaction was carried out, M is the slope, which indicates the catalytic activity of enzyme, and C is the intercept on the Y-axis. The slope of the absorbance fitted line (Fig. 5a) of free GOx ($y = 0.003x + 0.225$) and GOx-ALG-NCs ($y = 0.003x + 0.340$) was found to be similar, indicating that entrapped enzyme had similar catalytic activity as free GOx enzyme [43]. Figure 5b exhibited the effect of different pHs on the relative activity of enzymes in GOx-ALG-MCNPs. Curve a and b exhibited in Figure 5b show that maximum enzyme activity is observed at pH 5.8 and deactivation occurs at pH 2.1. Lesser enzyme activity (5.4%) was observed at pH 9.1. It reveals that GOx-ALG-MCNPs maintain the significant activity of enzymes similar to free enzymes in variable pH. A similar finding was also reported by Cheng et al [44]. It reveals that GOx-ALG-MCNPs maintain the significant activity of enzymes similar to free enzymes in the range of pH 4 - 8.

Estimation of glucose sensitivity

The effect of sugar concentration on the size of MCNPs, GOx-MCNPs, and GOx-ALG-MCNPs is exhibited in Figure 6a. The different concentration of sugar solution 100 - 250 mg/dL was prepared to correlate the effect of normal and elevated blood sugar level on the prepared system. Changes in the hydrodynamic radius and erosion of polymer are pH-dependent. The pH of the formulation is regulated by an enzymatic reaction between glucose and entrapped enzymes. On increasing glucose concentration in solution, a concentration gradient builds across the system which regulates glucose diffusion. The formation of gluconic acid is completely based on the availability of enzymes. The lowering in pH is governed by the amount of gluconic acid. The lower pH or acidic environment induced swelling and erosion in the system. The MCNPs without enzyme does not show swelling in variable glucose concentration (100, 150, 200, and 250 mg/dL) (Fig. 5a). A system that consists of enzymes (GOx-MCNPs and GOx-ALG-MCNPs) showed variable swelling properties when placed in different glucose concentrations (100, 150, 200, and 250 mg/dL). The hydrodynamic radius of GOx-MCNPs abruptly increases indicating that the system swells rapidly and shows burst release at all concentrations; it reveals that this system may cause a hypoglycemic effect on administration. However, GOx-ALG-MCNPs in 100 and 150 mg/dL of glucose solutions do not swell; it reveals that this system may not cause hypoglycemic effects under normal blood glucose levels. The hydrodynamic radius increases rapidly above 250 mg/dL due to the swelling of GOx-ALG-MCNPs. The alteration in hydrodynamic radius depends on glucose concentration; the immobilization of the enzyme plays a significant role in the regulation of pH and swelling behavior of NPs. The immobilization of the enzyme controls the formation of gluconic acid as compared to the free enzyme [13]; this results in poor swelling of NPs at 150 mg/dL and controlled swelling of GOx-ALG-MCNPs NPs at higher blood glucose levels.

Glucose-dependent effect of pH

The release of drugs from the system is regulated by pH change. The lowering of pH occurs as a result of the formation of gluconic acid, which is confirmed by the study of pH change. The prepared systems GOx-MCNPs and GOx-ALG-MCNPs were incubated with different strengths of glucose solution. Phosphate buffer pH 7.4 was used as a control solution. Figure 6b exhibited that S1 was not shown any significant changes in the pH of the solution at any glucose concentration (400 mg/dL). It reveals that the conversion of glucose into gluconic acid is the feature of glucose oxidase. The pH remains unchanged possibly due to the lack of an enzyme in the system. S2 and S3 show characteristic pH changes in the 100 and 400 mg/dL glucose solution. The pH of S2 and S3 reduced up to 2.1 folds (from pH 7.4 to 3.5) in 8 h and 6 h, respectively. The rate of pH change was rapid in initial duration (S2: 4 h, S3: 2 h), with the passage of time rate of pH change becomes low, which indicates the retardation of enzyme activity at lower pH. The optimum enzyme activity occurs at pH 4 - 7. The immobilization of the enzyme in a polymeric carrier controls the pH change which affects the swelling and releases properties. The S4 and S5 did not show any significant change in the pH of

the solution as compared to S1, S2, and S3; it exhibited that polymeric immobilization controls the enzymatic reaction. In S4 and S5, pH change was observed only at a higher concentration of glucose (400 mg/dL). The reduction of pH in S4 was not significant due to the low concentration of glucose (100 mg/dL). Similarly, Wang et al [15] also depicted the effect of glucose concentration on pH change.

Ex vivo mucoadhesion and cellular uptake study

GOx-ALG-MCNPs were applied over the freshly excised intestinal tissue (Fig. 7). The sample was applied over the excised layer and washed continuously with a pH 7.4 solution for 30 min and it was observed that GOx-ALG-MCNPs very well adhered to the mucosal layer of the intestine. No significant changes were observed in the intestine segment after washing; less than 10% amount of GOx-ALG-MCNPs were washed out during this study, which indicated that the formulation had good mucoadhesive properties. The percent of mucoadhesion was 94%. Mucoadhesion and absorption of NPs depend on ionic interaction with the intestinal membrane. Extended adherence of NPs over the mucosal surface was the key factor in cellular uptake of the system [45]. In the histopathological study, Figure 8a exhibited payer patches, and Figure 8b exhibited the appearance of microvilli. The tissue is compactly packed and lymph nodes are appearing in normal size. In Figure 8c, CNPs-treated mice (histopathological study) exhibited little dilation in microvilli tissue. Chitosan is a mucoadhesive polymer; it exhibits electrostatic interaction with negatively charged mucin molecules of the intestinal mucosa [46]. Figure 8d-f exhibited more dilation and inflammation in lymphoid tissue. It may occur due to the mucoadhesion characteristics of chitosan and receptor-mediated endocytosis of mannose ligand. Mannose selectively binds with the carbohydrate-binding receptor and is internalized through gut-associated lymphoid tissue via receptor-mediated endocytosis.

In vitro insulin release profile

Percentage insulin release was determined at three different pHs (1.2, 6.8, and 7.4) and variable glucose concentrations (0, 100, 200, and 400 mg/dL), simulated to physiological conditions. The pH of 7.4 was simulated to blood plasma condition, and the release was determined with or without the influence of glucose concentration (Fig. 8). No significant release of insulin in gastric fluid (pH 1.2) was observed because an enteric-coated shell prevents the disintegration of the capsule under acidic conditions [47]. The capsule reached the intestinal part after 2 h and disintegrated under the influence of alkaline pH. All the formulations were kept at 6.8 pH for 8 h, but no significant amount of insulin was released from MCNPs, GOx-MCNPs, and GOx-ALG MCNPs (Fig. 8). It inferred that erosion of chitosan was a pH-dependent phenomenon; it will ionize only under acidic conditions but resist dissolution under alkaline pH. As a result, NPs maintain their integrity and resist the insulin release in the intestine [48]. Mannosylated chitosan interacted with mucus membrane to allow para-cellular uptake through redistribution of F-actin and tight junction protein as also reported by Boroumand et al [49]. Similarly, NPs reach into the systemic circulation by cellular transport. To characterize the bio-responsive behavior of NPs, a release study was performed in different glucose concentrations (0, 100, 200, and 400 mg/dL), and the pH of the system was adjusted to 7.4. No significant insulin release was observed in absence of glucose solution; GOx-MCNPs released more than 95% insulin at all glucose concentrations (100, 200, and 400 mg/dL), suggesting that GOx-MCNPs were unable to control the release of insulin with respect to glucose concentration. This inferred that GOx freely reacts with glucose and forms gluconic acid, which rapidly decreases the pH of the system and causes ionization and erosion of the polymer. In GOx-ALG-MCNPs enzyme was entrapped in a multilayer of chitosan and alginate layer, which controlled the formation of gluconic acid by an enzymatic reaction. The release study reveals that the release of insulin from GOx-ALG-MCNPs depends on the concentration gradient of glucose. At a low concentration, (< 200 mg/dL) system retards pH change or release of insulin; however, at a high concentration gradient (> 200 mg/dL) pH decreases and the system promotes the release of insulin (Fig. 9).

In vivo study/blood glucose lowering effect

Figure 10 shows the changes in blood glucose levels upon administration of different formulations and insulin, orally as well as subcutaneously. Insulin-loaded GOx-MCNPs reduced the level of blood glucose from 400 to 217, 103, and 63 mg/dL at the doses of (50, 100, and 150) IU/kg body weight, respectively, within 3 h and reached the basal level within 8 - 9 h. The better glucose-lowering effect indicated the greater absorption; but the hypoglycemic effect at a higher dose (150 IU/Kg) indicates a lack of control release and bio-responsive properties. However, The GOx-ALG-MCNPs with the dose of insulin of 50, 100 and 150 IU/kg reduces the blood glucose level from 400 to 221, 107 and 103 mg/dL and return to the normal range within 17 - 18 h, reveling that GOx-ALG-MCNPs prevent the hypoglycemic condition at any dose. The triggering of enzymes and the release of insulin are controlled by multilayer covering and cross-linking [50]. Different insulin strength (100 and 150 IU/kg body weight) of GOx-ALG-MCNPs showed controlled blood sugar regulation, which indicated that the driving force behind the release of insulin is the concentration of enzyme (into the system) and substrate (blood glucose); amount of insulin present in the system does not affect the release. The rate-limiting step of the developed system is blood sugar concentration. Orally fed 50 IU/kg body weight dose of insulin solution was incapable to show noticeable effects in comparison with other NPs. On the contrary, subcutaneous injection of insulin at 5 IU/kg body weight dose showed an instantaneous hypoglycemic effect in the first hour and ultimately reaches the basal blood glucose level within the next 2 h. Saline-treated diabetic mice did not show any significant change in blood glucose level during the long fasting time. It also eliminated the probabilities of any influence in the reduction of blood glucose levels.

Conclusions

In this study, a biodegradable glucose-sensitive NPs system was formulated. Formulations were protected from the gastric environment and targeted into the intestinal part with the help of an acid-resistance enteric capsule shell. Formulation got absorbed from the intestine with the help of a mucoadhesive polymer and ligand. Mannose ligand plays an important role in cellular uptake via receptor-mediated endocytosis. Alginate nanocarrier significantly entrapped the enzyme and maintain its integrity and activity. SEM morphological study confirms their uniform shape and nano-sized structure. Nanostructured favored internalization of NPs. Dynamic swelling behavior of GOx-ALG-MCNPs with respect to glucose concentration and pH represents their bio-responsive characteristics. Mucoadhesion study confirms the retention property of NPs and the dilated lymphoid tissue observed in the histopathological study favors the internalization of the GOx-ALG-MCNPs. *In vitro* evaluations showed that the release of insulin from the system depends on glucose and pH. The *in vivo* study suggests that GOx-ALG-MCNPs significantly lower the blood glucose on oral administration and also prevent the chance of hypoglycemia at a higher dose. The release of insulin from the formulation is regulated by blood sugar level and the release was controlled by the degree of cross-linking. The GOx-ALG-NCs, chitosan polymer, and mannose ligand make the system efficient for oral administration and glucose-responsive insulin delivery.

Acknowledgments

This research work is supported by TEQIP-III, and School of Pharmaceutical Sciences, RGPV, Bhopal MP. India.

Financial Disclosure

Financial support of Rupee 3 lac was granted to coauthor Suman Ramteke and Pranay Guru from TEQIP-III, RGPV, under sanction order RGPV/TEQIP-III/2019/04/624.

Conflict of Interest

The authors do not have any conflict of interest.

Informed Consent

Not applicable.

Author Contributions

Rahul Maurya contributed substantially to the design of hypotheses, experiments, analysis, and drafting of manuscripts. Suman Ramteke and NK Jain have substantially contributed to the revising of manuscript content and Pranay Guru was also involved in the documentation of the grant.

Data Availability

The data supporting the findings of this study are available from the corresponding author upon reasonable request.

References

1. Rege NK, Phillips NFB, Weiss MA. Development of glucose-responsive 'smart' insulin systems. Curr Opin Endocrinol Diabetes Obes. 2017;24(4):267-278.
2. Wei Q, Qi L, Lin H, Liu D, Zhu X, Dai Y, et al. Pathological mechanisms in diabetes of the exocrine pancreas: what's known and what's to know. Front Physiol. 2020;11:570276.
3. Zaccardi F, Webb DR, Yates T, Davies MJ. Pathophysiology of type 1 and type 2 diabetes mellitus: a 90-year perspective. Postgrad Med J. 2016;92(1084):63-69.
4. Wang X, Wang H, Zhang T, Cai L, Kong C, He J. Current knowledge regarding the interaction between oral bone metabolic disorders and diabetes mellitus. Front Endocrinol (Lausanne). 2020;11:536.
5. Penfornis A, Personeni E, Borot S. Evolution of devices in diabetes management. Diabetes Technol Ther. 2011;13(Suppl 1):S93-102.
6. Moser E, Crew L, Garg S. Role of continuous glucose monitoring in diabetes management. Av en Diabetol. 2010;26(2):73-78.
7. Brazg RL, Bailey TS, Garg S, Buckingham BA, Slover RH, Klonoff DC, Nguyen X, et al. The ASPIRE study: design and methods of an in-clinic crossover trial on the efficacy of automatic insulin pump suspension in exercise-induced hypoglycemia. J Diabetes Sci Technol. 2011;5(6):1466-1471.
8. Gradel AKJ, Porsgaard T, Lykkesfeldt J, Seested T, Gram-Nielsen S, Kristensen NR, Refsgaard HHF. Factors affecting the absorption of subcutaneously administered insulin: effect on variability. J Diabetes Res. 2018;2018:1205121.
9. Sonia TA, Sharma CP. An overview of natural polymers for oral insulin delivery. Drug Discov Today. 2012;17(13-14):784-792.
10. Fuchs J, Hovorka R. Benefits and Challenges of Current Closed-Loop Technologies in Children and Young People With Type 1 Diabetes. Front Pediatr. 2021;9:679484.
11. Saeed M, Elshaer A. Glucose-sensitive materials for delivery of antidiabetic drugs. Engineering Drug Delivery Systems: Elsevier; 2020. p. 203-228.
12. Chia CW, Saudek CD. Glucose sensors: toward closed loop insulin delivery. Endocrinol Metab Clin North Am. 2004;33(1):175-195.
13. Jamwal S, Ram B, Ranote S, Dharela R, Chauhan GS. New glucose oxidase-immobilized stimuli-responsive

dextran nanoparticles for insulin delivery. Int J Biol Macromol. 2019;123:968-978.
14. Huang Q, Wang L, Yu H, Ur-Rahman K. Advances in phenylboronic acid-based closed-loop smart drug delivery system for diabetic therapy. J Control Release. 2019;305:50-64.
15. Wang J, Wang Z, Yu J, Kahkoska AR, Buse JB, Gu Z. Glucose-responsive insulin and delivery systems: innovation and translation. Adv Mater. 2020;32(13):e1902004.
16. Alqahtani MS, Kazi M, Alsenaidy MA, Ahmad MZ. Advances in oral drug delivery. Front Pharmacol. 2021;12:618411.
17. Hu J, Wei P, Seeberger PH, Yin J. Mannose-Functionalized Nanoscaffolds for Targeted Delivery in Biomedical Applications. Chem Asian J. 2018;13(22):3448-3459.
18. Patil TS, Deshpande AS. Mannosylated nanocarriers mediated site-specific drug delivery for the treatment of cancer and other infectious diseases: A state of the art review. J Control Release. 2020;320:239-252.
19. Opanasopit P, Higuchi Y, Kawakami S, Yamashita F, Nishikawa M, Hashida M. Involvement of serum mannan binding proteins and mannose receptors in uptake of mannosylated liposomes by macrophages. Biochim Biophys Acta. 2001;1511(1):134-145.
20. Smart JD. The basics and underlying mechanisms of mucoadhesion. Adv Drug Deliv Rev. 2005;57(11):1556-1568.
21. Ma Z, Lim TM, Lim LY. Pharmacological activity of peroral chitosan-insulin nanoparticles in diabetic rats. Int J Pharm. 2005;293(1-2):271-280.
22. Ganaie MA, Rawat HK, Wani OA, Gupta US, Kango NJPB. Immobilization of fructosyltransferase by chitosan and alginate for efficient production of fructooligosaccharides. Process Biochem. 2014;49(5):840-844.
23. Tantra R, Schulze P, Quincey PJP. Effect of nanoparticle concentration on zeta-potential measurement results and reproducibility. Particuology. 2010;8(3):279-285.
24. Ein Ali Afjeh M, Pourahmad R, Akbari-Adergani B, Azin MJFS. Characteristics of glucose oxidase immobilized on Magnetic Chitosan Nanoparticles. Food Sci Technol. 2019;40:68-75.
25. Chen Y, Furmann A, Mastalerz M, Schimmelmann AJF. Quantitative analysis of shales by KBr-FTIR and micro-FTIR. Fuel.2014;116:538-549.
26. Bhattacharyya A, Mukherjee D, Mishra R, Kundu PP-JEPJ. Preparation of polyurethane-alginate/chitosan core shell nanoparticles for the purpose of oral insulin delivery. Eur Poly J. 2017;92:294-313.
27. Du X, Zhang T, Ma G, Gu X, Wang G, Li J. Glucose-responsive mesoporous silica nanoparticles to generation of hydrogen peroxide for synergistic cancer starvation and chemistry therapy. Int J Nanomedicine. 2019;14:2233-2251.
28. Sonaje K, Chen YJ, Chen HL, Wey SP, Juang JH, Nguyen HN, Hsu CW, et al. Enteric-coated capsules filled with freeze-dried chitosan/poly(gamma-glutamic acid) nanoparticles for oral insulin delivery. Biomaterials. 2010;31(12):3384-3394.
29. Kiilll CP, Barud HDS, Santagneli SH, Ribeiro SJL, Silva AM, Tercjak A, Gutierrez J, et al. Synthesis and factorial design applied to a novel chitosan/sodium polyphosphate nanoparticles via ionotropic gelation as an RGD delivery system. Carbohydr Polym. 2017;157:1695-1702.
30. Goycoolea FM, Lollo G, Remunan-Lopez C, Quaglia F, Alonso MJ. Chitosan-alginate blended nanoparticles as carriers for the transmucosal delivery of macromolecules. Biomacromolecules. 2009;10(7):1736-1743.
31. Hassani S, Laouini A, Fessi H, Charcosset CJC, Physicochemical SA, Aspects E. Preparation of chitosan-TPP nanoparticles using microengineered membranes-Effect of parameters and encapsulation of tacrine. Colloids Surf A: Physicochem Eng Asp. 2015;482:34-43.
32. Liu G, Zhou Y, Chen L. Intestinal uptake of barley protein-based nanoparticles for beta-carotene delivery. Acta Pharm Sin B. 2019;9(1):87-96.
33. Melo MN, Pereira FM, Rocha MA, Ribeiro JG, Diz FM, Monteiro WF, et al. Immobilization and characterization of Horseradish Peroxidase into Chitosan and Chitosan/PEG nanoparticles: A comparative study. Process Biochem. 2020;98:160-171.
34. Zhang YW, Tu LL, Tang Z, Wang Q, Zheng GL, Yin LN. pH-sensitive chitosan-deoxycholic acid/alginate nanoparticles for oral insulin delivery. Pharm Dev Technol. 2021;26(9):943-952.
35. Alasonati E, Caebergs T, Petry J, Sebaihi N, Fisicaro P, Feltin N. Size measurement of silica nanoparticles by Asymmetric Flow Field-Flow Fractionation coupled to Multi-Angle Light Scattering: A comparison exercise between two metrological institutes. J Chromatogr A. 2021;1638:461859.
36. Dhanasekaran S, Rameshthangam P, Venkatesan S, Singh SK, Vijayan SRJJoP, Environment T. In vitro and in silico studies of chitin and chitosan based nanocarriers for curcumin and insulin delivery. J Polym Environ. 2018;26(10):4095-4113.
37. Shibaguchi K, Tamura A, Terauchi M, Matsumura M, Miura H, Yui NJM. Mannosylated polyrotaxanes for increasing cellular uptake efficiency in macrophages through receptor-mediated endocytosis. Molecules. 2019;24(3):439.
38. Pavia DL, Lampman GM, Kriz GS, Vyvyan JA. Introduction to spectroscopy: Cengage learning; 2014.
39. Asthana GS, Asthana A, Kohli DV, Vyas SP. Mannosylated chitosan nanoparticles for delivery of antisense oligonucleotides for macrophage targeting. Biomed Res Int. 2014;2014:526391.
40. Chai Z, Dong H, Sun X, Fan Y, Wang Y, Huang F. Development of glucose oxidase-immobilized alginate nanoparticles for enhanced glucose-triggered insulin delivery in diabetic mice. Int J Biol Macromol. 2020;159:640-647.
41. Jing H, Huang X, Du X, Mo L, Ma C, Wang H. Facile synthesis of pH-responsive sodium alginate/carboxymethyl chitosan hydrogel beads promoted by hydrogen bond. Carbohydr Polym. 2022;278:118993.
42. Janati-Fard F, Housaindokht MR, Monhemi H, Esmaeili AA, Nakhaei Pour A. The influence of two imidazolium-based ionic liquids on the structure and activity of glucose

oxidase: Experimental and theoretical studies. Int J Biol Macromol. 2018;114:656-665.
43. Baruch-Shpigler Y, Avnir D. Entrapment of glucose oxidase within gold converts it to a general monosaccharide-oxidase. Sci Rep. 2021;11(1):10737.
44. Cheng K, Zhang Y, Li Y, Gao Z, Chen F, Sun K, et al. A novel pH-responsive hollow mesoporous silica nanoparticle (HMSN) system encapsulating doxorubicin (DOX) and glucose oxidase (GOX) for potential cancer treatment. J Mater Chem B. 2019;7(20):3291-3302.
45. Cao SJ, Xu S, Wang HM, Ling Y, Dong J, Xia RD, Sun XH. Nanoparticles: Oral Delivery for Protein and Peptide Drugs. AAPS PharmSciTech. 2019;20(5):190.
46. Samprasit W, Opanasopit P, Chamsai B. Mucoadhesive chitosan and thiolated chitosan nanoparticles containing alpha mangostin for possible Colon-targeted delivery. Pharm Dev Technol. 2021;26(3):362-372.
47. Gracia R, Yus C, Abian O, Mendoza G, Irusta S, Sebastian V, Andreu V, et al. Enzyme structure and function protection from gastrointestinal degradation using enteric coatings. Int J Biol Macromol. 2018;119:413-422.
48. Fang Y, Wang Q, Lin X, Jin X, Yang D, Gao S, Wang X, et al. Gastrointestinal responsive polymeric nanoparticles for oral delivery of insulin: optimized preparation, characterization, and in vivo evaluation. J Pharm Sci. 2019;108(9):2994-3002.
49. Boroumand H, Badie F, Mazaheri S, Seyedi ZS, Nahand JS, Nejati M, Baghi HB, et al. Chitosan-based nanoparticles against viral infections. Front Cell Infect Microbiol. 2021;11:643953.
50. Ghiorghita CA, Bucatariu F, Dragan ES. Influence of cross-linking in loading/release applications of polyelectrolyte multilayer assemblies. A review. Mater Sci Eng C Mater Biol Appl. 2019;105:110050.